Quantum Chemical Studies of the Structures and Vibrations of Trisilylmethane and Tetrasilylmethane

Donald C. McKean*

School of Chemistry, University of Edinburgh, West Mains Road, Edinburgh EH9 3JJ, U.K.

Received: September 22, 2003; In Final Form: March 3, 2004

Quantum chemical studies of trisilylmethane, $(SiH_3)_3CH$, (TSM) and tetrasilylmethane, $(SiH_3)_4C$, (TTSM) have been made by the HF, MP2, and B3LYP methods. The silyl groups in each compound are twisted through 12−20° from the completely staggered configurations, yielding the point groups C_3 (TSM) and T (TTSM), respectively, in fair agreement with electron diffraction results. Structures have also been calculated for the higher energy, fully staggered configurations. These exhibit H···H distances between neighboring silyl groups, which are significantly less than those in the staggered, equilibrium structures calculated for disilylmethane (DSM). In a survey of QC-based torsional frequencies in molecules containing silyl groups, TSM, TTSM, and DSM are exceptional in exhibiting marked variations in their calculated in-phase torsional frequencies according to the computational method employed. In TSM and TTSM, MP2 values are much larger than B3LYP ones, reflecting similar differences in internal rotation barrier. This may be due to the longer bond lengths and nonbonded H···H distances yielded by the DFT method. QC-based vibration frequencies and overall intensities of SiH and CH stretching bands in TSM and TTSM are scaled using earlier experimental data from related compounds such as DSM. Agreement with the sparse infrared data currently available for condensed phases is only fair. Electrical properties of the Si−H and C−H bonds are compared with those of related silyl compounds. Infrared intensities of CH and SiH stretching bands show the expected behavior due to inductive effects on the charges on the H atoms involved.

Introduction

Trisilylmethane (TSM) and tetrasilylmethane (TTSM) were prepared for the first time quite recently, and their structures were determined by gas-phase electron diffraction (ED).[1,2] Interest in these compounds was both structural and technological. Rotation of the silyl groups away from the staggered configuration present in their carbon analogues of isobutane and isopentane seemed likely, while the use of such compounds in chemical vapor deposition of thin films merited exploration.[1,2] Both ED studies showed a rotation of the silyl groups through about 20° from a staggered conformation. Theoretical confirmation of this rotation is to be desired.

A few infrared bands have been reported from films of TSM[3] and TTSM[2], but no detailed spectral study as yet exists. The closely related molecule of disilylmethane (DSM) has recently been the subject of a combined infrared and quantum chemical (QC) study,[4] the results of which pointed to a need for similar QC work on TSM and TTSM.

One feature of this prior study of DSM was a marked variation in the value predicted for the lower of the two silyl torsional modes, $\nu_{14}(a_2)$, from the different levels of theory. MP2 calculations gave much lower values than HF or B3LYP ones, such that very large scale factors were needed if the experimental value was to be reproduced. (This experimental value was obtained from overtone and combination bands involving SiH stretching.) By contrast, the HF and B3LYP predictions appeared to be quite reasonable. The reason for this anomalous behavior of the MP2 calculation was unclear, and it is natural to enquire whether similar variations in predicted torsional frequency appear in the present molecules, TSM and TTSM, although no experimental data are as yet available. No such variation is found in calculations for molecules containing only a single silyl group.[4]

A further feature of this DSM work was the determination of a large number of scale factors for the QC-based symmetry force constants. If these scale factors could be transferred to TSM and TTSM, a fairly precise prediction of the spectra of these two compounds might be achieved, which would guide much needed new experimental work.

QC studies are also useful in demonstrating the changes that occur in bond and atom properties such as isolated stretching frequencies, ν^{is}CH and ν^{is}SiH, and their band intensities, as well as dipole derivatives and electric charges of various kinds on the atoms concerned. Comparisons of such quantities between molecules must of course be carried out using a common level of theory. Several such studies have been reported for silyl compounds using density functional theory in the B3LYP approach with the basis set 6-311G**.[4,5]

Theoretical Details

Calculations were performed with the program Gaussian 98,[6] as in previous work from this laboratory.[4] The methods employed were HF, MP2, and B3LYP in conjunction with the basis sets 6-31G* (hereafter "sv" (split valence)) and 6-311G** (hereafter "tz" (triple-ζ)). Some calculations were also carried out with the addition of diffuse functions, the basis sets then being 6-31++G* (hereafter "sv+") and 6-311++G** (hereafter "tz+"). Structures were optimized with the "tight" condition for convergence, to minimize rounding errors in small differences in structural parameters. Initially, the symmetries of the

* E-mail: dmckean@staffmail.ed.ac.uk.

10.1021/jp0310807 CCC: $27.50
Published on Web 05/01/2004

TABLE 1: Bond Lengths, Bond Angles, Dipole Moments, and Torsional Frequencies for the Equilibrium (C_3) Structure of Trisilylmethane and Relative Energies of the C_3 and C_{3v} Forms[a]

parameter[b]	HF/sv	HF/tz	MP2/sv	MP2/ sv+	MP2/tz	MP2/ tz+	B3LYP/sv	B3LYP/sv+	B3LYP/tz	B3LYP/tz+	obsd[c]
rC−H	1.0919	1.0923	1.0988	1.1005	1.0991	1.0993	1.1004	1.1015	1.0987	1.0987	1.100[d]
rSi−C	1.8912	1.8900	1.8843	1.8855	1.8824	1.8827	1.8924	1.8933	1.8934	1.8932	1.878(1)
rSi−H[a]	1.4772	1.4797	1.4870	1.4863	1.4786	1.4792	1.4880	1.4872	1.4862	1.4864	1.497(3)
rSi−H[b]	1.4766	1.4786	1.4867	1.4858	1.4774	1.4778	1.4883	1.4876	1.4861	1.4862	1.497[e]
rSi−H[c]	1.4777	1.4802	1.4880	1.4872	1.4792	1.4796	1.4893	1.4887	1.4873	1.4875	1.497[e]
∠HCSi	106.33	105.84	107.64	107.42	106.92	107.00	106.87	106.72	106.24	106.29	107.8(2)
∠H[a]SiC	110.20	110.23	109.53	109.46	109.40	109.32	110.15	110.10	110.09	110.07	108.7(7)
∠H[b]SiC	110.36	110.27	110.58	110.46	110.32	110.38	110.55	110.44	110.36	110.36	108.7[e]
∠H[c]SiC	110.99	110.79	111.08	111.09	110.84	110.87	111.16	111.06	110.87	110.87	108.7[e]
τH[a]SiCH	165.29	165.14	163.18	164.36	163.46	163.08	168.32	168.48	168.48	167.20	158.3(18)
τH[b]SiCH	45.41	45.22	43.43	44.68	43.73	43.34	48.47	48.64	48.61	47.32	38.3[e]
τH[c]SiCH	−74.82	−74.98	−77.19	−76.01	−76.98	−77.40	−71.77	−71.62	−71.66	−72.96	−81.7[e]
μ	0.712	0.676	0.774	0.767	0.718	0.714	0.697	0.704	0.671	0.658	
ν_{12} (a)	112.3	109.1	145.0	128.0	129.9	na[f]	86.0	82.9	76.0	86.7	
ν_{24} (e)	115.7	111.0	124.0	120.6	114.6	na[f]	113.1	112.5	105.9	104.5	
$\Delta E(C_{3v}-C_3)$	0.70	0.67	1.66	1.06	1.25	1.64	0.27	0.24	0.20	0.32	

[a] Units: bond lengths r in angstroms; angles ∠, τ in degrees; energy differences ΔE in kJ mol^{-1}; dipole moments μ in Debye; torsional frequencies τ in cm^{-1}. [b] In Figure 1, atoms H(6), H(9), and H(12) are H[a]; H(7), H(10), and H(13) are H[b]; H(8), H(11), and H(14) are H[c]. [c] Reference 1. [d] Assumed. [e] Constrained by the assumption of C_{3v} local symmetry for each silyl group. [f] na = not available.

two molecules were constrained to the point groups C_3 (TSM) and T (TTSM) found experimentally. In all cases where frequencies were also obtained, these proved to be equilibrium structures. The geometries and energies of the fully staggered C_{3v} (TSM) and T_d structures (TTSM) were also calculated, as was an eclipsed T_d structure for TTSM.

The vibrational force field for TSM was scaled by use of the program ASYM40[7] with scale factors transferred from DSM.[4] This entailed using similar types of symmetry coordinates in TSM to those employed in DSM, which are listed in the Supporting Information, Table 1S. This in turn meant adopting the procedure devised by Cyvin et al.[8] for handling the vibrations of E species for a point group such as C_3 where complex symmetry coordinates are strictly necessary. (This procedure was recently used for trisilylamine.[9]) Even with similar types of symmetry coordinates, problems in the transfer of the scale factors remained, as outlined below. The Cyvin procedure is not applicable to the case of the triply degenerate coordinate sets needed in TTSM, and thus for this molecule a simpler type of correction, described below, was applied to the computed frequencies.

With one exception, calculations were performed on a DEC Alpha 1000 work station. However, the MP2/6-311G** frequency job required the use of Columbus, the DEC 8400 superscalar cluster equipped with 10 fast processors, 6 GB of memory, and a 150 GB disk, available at the U.K. Computational Chemistry Facility.

Results

Geometry and Torsional Frequencies. Figures 1 and 2 show the calculated equilibrium C_3 and T structures and atom numbering for TSM and TTSM, respectively. The corresponding geometric parameters for the ranges of QC calculations are contained in Tables 1 and 2, respectively, and compared with the previously observed ED values. Also given in these tables are the calculated torsional frequencies τ and the energy differences ΔE between equilibrium and staggered structures. For TTSM, ΔE for the eclipsed structure is also included. Geometries of the staggered structures of TSM and TTSM are available in the Supporting Information Tables 2S and 3S.

Agreement between calculated and observed values on the amount of twist of the silyl groups away from the staggered C_{3v} or T_d structures is quite good. In TSM, the observed twist

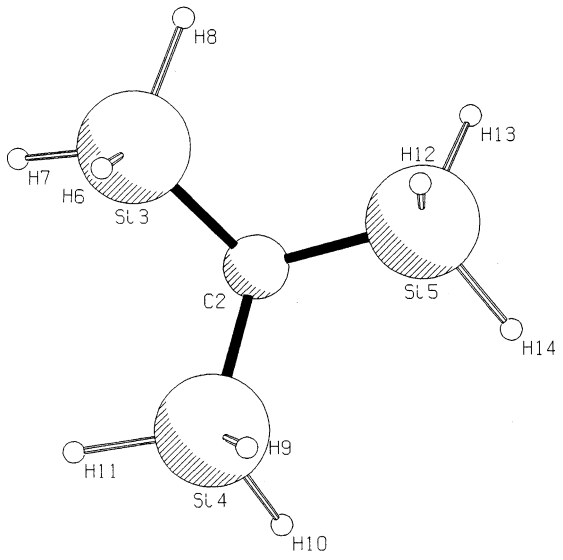

Figure 1. C_3 structure of trisilylmethane, from MP2/6-311G** calculations. H(1) is hidden behind C(2). The dihedral angle H(6)Si(3)C(2)H(1) is 163.5°, corresponding to a twist of the silyl group through about 16.5° from a staggered C_{3v} conformation.

of about 22° is best reproduced by the MP2 calculations (∼17°), worst by the B3LYP ones (∼12°). In TTSM, the triple-ζ calculations of the HF and MP2 twist angles of 19.5° and 19.6°, respectively, agree excellently with the observed value of 20(1)°. The corresponding B3LYP twist of 17.1° is a little low. A systematic difference between calculated and observed data occurs in respect of the HSiC angles in both molecules, the theoretically based ones being larger by up to 2°.

The most striking feature of the calculations in Tables 1 and 2 is the variability of the torsional frequencies with the method used. In TSM, the in-phase frequency ν_{12}(a) is 1.5 to 1.7 times greater from the MP2 model than it is from the B3LYP one, with the HF values lying in between. The calculated values of ν_{24} are more similar, but here again the MP2 values tend to be higher. By comparison, the effects of basis set are quite minor. There is a clear link between the variability of ν_{12} and the energy ΔE needed to stagger the silyl groups fully. The latter is only ∼0.3 kJ mol^{-1} in the B3LYP calculations but 1.1 to 1.7 kJ mol^{-1} in the MP2 ones. The mode ν_{12} is, of course, the one that leads to the T_d configuration. That the calculational method employed

TABLE 2: Bond Lengths, Bond Angles, Dipole Moments, and Torsional Frequencies for the Equilibrium (*T*) Structure of Tetrasilylmethane and Relative Energies of the *T* and T_d Staggered (st) or Eclipsed (ec) Forms[a]

parameter	HF/sv	HF/tz	MP2/sv	MP2/sv+	MP2/tz	MP2/tz+	B3LYP/sv	B3LYP/sv+	B3LYP/tz	B3LYP/tz+	obsd[b]
*r*Si−C	1.8948	1.8964	1.8844	1.8863	1.8852	1.8853	1.8947	1.8960	1.8983	1.8982	1.8751(7)
*r*Si−H	1.4768	1.4793	1.4877	1.4870	1.4791	1.4797	1.4884	1.4876	1.4866	1.4868	1.486(4)
∠HSiC	110.49	110.38	110.32	110.23	110.09	110.06	110.56	110.46	110.36	110.34	108.5(6)
τHSiCSi[c]	161.37	160.50	160.61	162.03	160.40	160.46	164.07	164.43	162.93	162.34	160.0(10)
ν_4(a)	182.6	189.3	203.1	na	192.8	na	130.4	132.8	134.8	na	
ν_{19}(t)	152.1	149.9	161.6	na	152.7	na	127.9	132.0	120.0	na	
ΔE (eq-st)	4.3	5.1	6.3	4.4	5.6	6.4	1.9	1.8	2.3	2.6	
ΔE (eq-ec)	58.2	56.4	58.2	62.8	53.4	na	50.6	52.1	47.7	na	

[a] Units: bond lengths *r* in Å; angles ∠, τ in degrees; energy difference ΔE in kJ mol^{-1}; silyl torsional frequencies ν_4(a) and ν_{19}(t) in cm^{-1}. [b] Reference 2. [c] This angle is 180.0° in the staggered T_d structure.

TABLE 3: Comparison of QC Values of Silyl Torsional Frequencies (cm^{-1}) in Some Silyl Compounds[a]

level	MS[b]	DS[b]	FMS[b]	CMS[b]	DSM[b]	DSM[b]	TSM	TSM	TTSM	TTSM
	ν_6(a_2)	ν_{12}(a_{1u})	ν_{18}(a″)	ν_{18}(a″)	ν_{14}(a_2)	ν_{27}(b_2)	ν_{12}(a)	ν_{24}(e)	ν_4(a)	ν_{19}(t)
HF/sv	193.6	133.0	157.6	157.2	69.1	144.0	112.3	115.7	182.6	152.1
HF/tz	197.9	134.7	154.5	158.9	75.7	142.6	109.1	111.0	189.3	149.9
MP2/sv	201.7	140.4	169.4	161.8	47.8	145.7	145.0	124.0	161.6	203.1
MP2/tz	196.0	147.6	158.1	159.9	56.7	139.0	129.9	114.6	192.8	152.7
B3LYP/sv	192.3	129.7	161.3	153.7	73.1	136.1	86.0	113.1	127.9	130.4
B3LYP/tz	193.9	135.4	154.4	155.5	81.0	136.3	76.0	105.9	120.0	134.8
B3LYP/tz+	192.4	131.5	151.0	154.0	77.9	135.2	86.7	104.5	na	na
obsd	190	125.5	149	161	78.5	133				

[a] MS = methylsilane, DS = disilane, FMS = fluoromethylsilane, CMS = chloromethylsilane. [b] From ref 4.

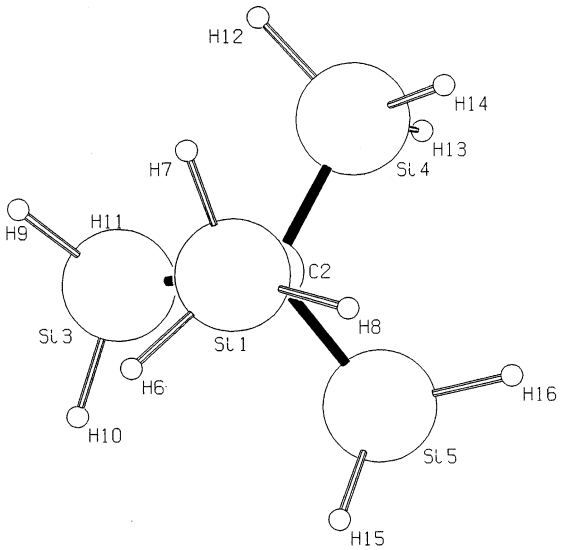

Figure 2. Structure of tetrasilylmethane (point group *T*) from MP2/6-311G** calculations. The dihedral angle H(6)Si(1)C(2)Si(4) is 160.4°, corresponding to a twist of the silyl group through 19.6° from a staggered T_d conformation.

is the source of differences in both torsional frequency and ΔE was indicated by a single BPW91/6-311G** calculation, which gave results virtually identical to those from the B3LYP model.

In TTSM, there is a similar variablility in the in- and out-of-phase torsions ν_4(a) and ν_{19}(t), respectively, and also in ΔE. ν_4 is much larger than ν_{19} in the HF and MP2 calculations, but the two are comparable in the B3LYP model. The change in ν_4 with level of theory is paralleled by the difference in ΔE, which is up to 4 kJ mol^{-1} greater from an MP2 calculation than it is from a comparable B3LYP one.

These variations due to method are on the same scale as, but in the opposite direction to, the changes in values calculated for the in-phase torsional mode ν_{14}(a_2) for DSM, included in Table 3. In DSM the MP2 values are much lower than the B3LYP ones, with the experimental evidence favoring the latter. In contrast, in TSM and to a lesser extent in TTSM, the MP2 results are slightly to be preferred since they yield twist angles closer to those observed by ED.

Also shown in Table 3 are the calculated torsional frequencies for methylsilane (MS), disilane (DS), fluoromethylsilane (FMS), and chloromethylsilane (CMS). In contrast with DSM, TSM, and TTSM, these show rather little variation with the QC method. This focuses attention on the interaction between two silyl groups separated by a single atom as the source of the variability in DSM, TSM, and TTSM.

A possible explanation for the effect may lie in differences in the calculated distances between the hydrogen atoms in differing silyl groups. Table 4 shows the shortest such distances in the C_{3v} structure of TSM (H_7-H_{11}, H_6-H_9, and H_6-H_{11}) and in the staggered T_d form of TTSM (H_6-H_{10} and H_6-H_9), together with the changes in these distances on passing to the equilibrium forms. Also shown is the shortest $H^a-H^{a'}$ distance between the two silyl groups in the C_{2v} equilibrium structure of DSM. This is about about 0.2 Å greater than the H_7-H_{11} distance in TSM or the H_6-H_{10} distance in TTSM, presumably due to the large SiCSi angle (∼114°) in DSM. This provides an obvious clue as to why the equilibrium structure of DSM remains fully staggered, whereas those of TSM and TTSM have instead undergone a silyl twist of 20−22°.

While both H_7-H_{11} and H_6-H_9 distances in TSM lengthen significantly on passing from the C_{3v} to the C_3 structure, a larger effect is found with the shorter H_7-H_{11} distance, as might be expected. It is also seen that the MP2 distances are shorter by about 0.02 Å than the B3LYP ones, with a concomitant greater lengthening on passing to the C_3 form. The same is true of the H_6-H_{10} distance in TTSM. The closer approach of the non-bonded H_7 and H_{11} (TSM) or H_6 and H_{11} (TTSM) atoms in the MP2 structures may therefore be the source of the higher MP2 torsional frequencies. However, it is odd that the torsional frequency anomaly is primarily associated with the in-phase "geared" motion which might be thought to be less sensitive to the proximity of the hydrogens than the out-of-phase one, where the SiH bonds tend to clash with each other.

Another possible factor in causing differences in QC-calculated torsional frequency and barrier height might be the

TABLE 4: Close H(Si$_i$)−H(Si$_j$) Distances (Å) in the Staggered Structures in DSM, TSM, and TTSM and Their Changes from Equilibrium to Staggered Conformation

	DSM[a]	TSM						TTSM			
	$H^a-H^{a'}$	H_7-H_{11}		H_6-H_9		H_6-H_{11}		H_6-H_{10}		H_6-H_9	
level		C_{3v}	C_3-C_{3v}	C_{3v}	C_3-C_{3v}	C_{3v}	C_3-C_{3v}	T_d	$T-T_d$	T_d	$T-T_d$
HF/sv	3.359	3.146	0.093	3.341	0.052	4.032	−0.507	3.142	0.130	3.951	−0.658
HF/tz	3.380	3.138	0.096	3.374	0.049	4.044	−0.514	3.142	0.141	3.954	−0.692
MP2/sv	3.277	3.136	0.118	3.248	0.054	4.002	−0.607	3.118	0.143	9.945	−0.693
MP2/sv+	3.294	3.136	0.102	3.261	0.039	4.006	−0.563	3.121	0.120	3.946	−0.644
MP2/tz	3.298	3.119	0.118	3.273	0.057	3.998	−0.586	3.107	0.147	3.930	−0.696
MP2/tz+	3.300	3.123	0.122	3.268	0.060	3.998	−0.603	3.108	0.144	3.932	−0.696
B3LYP/sv	3.334	3.155	0.060	3.309	0.026	4.033	−0.406	3.147	0.096	3.965	−0.567
B3LYP/sv+	3.342	3.151	0.059	3.320	0.022	4.036	−0.401	3.146	0.090	3.964	−0.555
B3LYP/tz	3.360	3.145	0.060	3.347	0.023	4.043	−0.400	3.146	0.108	3.964	−0.609
B3LYP/tz+	3.359	3.145	0.073	3.347	0.030	4.043	−0.447	3.145	0.115	3.964	−0.631

[a] H^a and $H^{a'}$ are on the same side of the skeletal plane.

TABLE 5: Mulliken Charges (e) on H(Si) Atoms in the Staggered Structures of DSM, TSM, and TTSM

	DSM[a]		TSM[a](C_{3v})		TTSM (T_d)
level	H^s	H^a	H^s	H^a	H
HF/sv	−0.146	−0.144	−0.136	−0.139	−0.129
HF/tz	−0.196	−0.193	−0.184	−0.188	−0.176
MP2/sv	−0.104	−0.102	−0.091	−0.096	−0.084
MP2/sv+	−0.072	−0.088	−0.072	−0.064	−0.043
MP2/tz	−0.165	−0.164	−0.153	−0.157	−0.144
MP2/tz+	−0.151	−0.151	−0.122	−0.136	−0.103
B3LYP/sv	−0.069	−0.069	−0.061	−0.064	−0.055
B3LYP/sv+	−0.042	−0.048	−0.027	−0.031	−0.005
B3LYP/tz	−0.133	−0.132	−0.122	−0.124	−0.113
B3LYP/tz+	−0.121	−0.119	−0.097	−0.111	−0.085

[a] H^s atoms lie on planes of symmetry, and H^a atoms lie above or below such planes.

size of the electric charge on the hydrogens involved. Table 5 shows the negative Mulliken charges on the H atoms in the Si−H bonds of the staggered structures of DSM, TSM, and TTSM. In any given molecule, the B3LYP charges are consistently smaller than the MP2 ones for the same basis set. However, the same difference in Mulliken charge is evident in the B3LYP and MP2 calculations for DSM where the latter give *lower* values of the torsional frequency $\nu_{14}(a_2)$, as seen in Table 3.

There has been interest in the past in the changes in geometry associated with internal rotation; for example, from staggered to eclipsed forms in molecules of the type H_3X-YH_3.[10,11] Although the equilibrium forms of TSM and TTSM are twisted only about one-third of the way from a staggered to an eclipsed configuration, it was thought worthwhile to compare the changes seen with those occurring in methylsilane (MS) on passing from the staggered C_{3v} to the eclipsed C_{3h} conformation. Full details of 10 calculations of C_{3v} and C_{3h} structures for MS are given in Table 4S of the Supporting Information. Common to all three molecules is a small increase in rSi−C with departure from the equilibrium configuration. However, while this increase is virtually independent of the model for MS, at about 0.01 Å, as in ref 10, for TSM and TTSM it is more variable. Average changes ΔrSi−C(st-eq) (Å) are: for TSM, 0.0006(HF), 0.0008-(MP2), and 0.0003(B3LYP); for TTSM, 0.0033(HF), 0.0034-(MP2), and 0.0023(B3LYP). In TTSM, ΔrSi−H(st-eq) is consistently negative, the range being −0.0005 to −0.0007 Å. This contrasts with an essentially zero change in rSi−H in MS.

HSiC angle changes are trivial in TTSM (<0.04°), but in TSM this angle and the HCSi one can vary up to 0.5° and 0.7°, respectively.

Predictions of Frequency and Intensity. *TSM*. Table 6 shows the unscaled data (frequencies, infrared, and Raman intensities) for TSM from the HF/tz, MP2/tz, and B3LYP/tz treatments, together with the scaled frequencies obtained by transfer of scale factors from DSM. In this transfer, the TSM silyl deformation factor was taken to be the average of the differing DSM $\delta_{as}SiH_3$ and δ_sSiH_3 factors, while for the δCH factor, the mean was taken of the δCH_2, τCH_2, ρCH_2, and wCH_2 factors in DSM. In addition, the DSM νSiH^a factor was used for all three types of SiH bond in TSM. The latter assumption will introduce slight errors in the prediction of νSiH_3 modes.

All three treatments agree on placing the scaled νCH ν_1 at about 2895 cm^{-1}. This is so far from any of the weak bands reported[3] at 2957, 2925, and 2855 cm^{-1} that all these bands must be overtones or combinations. The calculated values of infrared intensity for ν_1 are all very low. On the basis of comparisons between calculated B3LYP/tz and observed intensities in other molecules discussed below (Table 10), the observed intensity should be close to 0.5 km mol^{-1}, which is consonant with a failure to observe this mode.

In the νSiH region, experience with DSM indicates that MP2 or B3LYP predictions of νSiH are preferred over HF ones. The range of νSiH values (2172−2155 cm^{-1} from the B3LYP/tz treatment) brackets the observed film value of 2153 cm^{-1} when allowance is made for a frequency shift due to change of phase. Individual bands are unlikely to be resolved. The total observed infrared intensity should be about 730 km mol^{-1}.

The δCH mode ν_{16} is not well-predicted. A gas−film phase shift is unlikely to explain the difference between observed (1024 cm^{-1}) and predicted values (B3LYP, 1052; MP2, 1049 cm^{-1}). Clearly the transfer of a mean scale factor from DSM is unsatisfactory here. As an alternative, a δCH scale factor was transferred from analogous treatments of $CHCl_3$. The result was more satisfactory for the HF (1045 cm^{-1}) and MP2 (1034 cm^{-1}) treatments but less so for the B3LYP one (1061 cm^{-1}). This again illustrates the uncertainty involved in the transfer of scale factors from one molecule to another.

Predictions of the silyl deformation frequencies and of the $\nu_{as}CSi_3$ mode ν_{20} appear satisfactory, bearing in mind the likely gas−liquid frequency shifts involved and the overlap of bands in the 930 cm^{-1} region.

Application of the silyl rocking scale factors from DSM involves the difficulty of the substantial difference between the $\rho'SiH_3$ and $\rho''SiH_3$ factors there and the choice that has to be made as to which silyl rocking modes in TSM correspond to those in DSM. This has a marked influence on the prediction of the bands in the region 820−550 cm^{-1}. The mode most affected is ν_9(a), which from its spectral intensities and PED is closely related to the A_2 mode for a C_{3v} structure. Since this

TABLE 6: Unscaled and Scaled Vibrational Data for TSM

	HF/tz			MP2/tz		B3LYP/tz		HF/tz	MP2/tz	B3LYP/tz	obsd	
mode	ν_{unsc}[a]	A[b]	R[c]	ν_{unsc}[a]	A[b]	ν_{unsc}[a]	A[b]	ν_{sc}[a]	ν_{sc}[a]	ν_{sc}[a]	ν_{obsd}[d]	motion
ν_1(a)	3141	2	72	3088	0	3019	1	2898	2895	2896	?[e]	νCH
ν_2(a)	2343	8	674	2314	166	2234	255	2188	2169	2172		νSiH
ν_3(a)	2327	412	89	2312	147	2230	39	2173	2167	2167		νSiH
ν_{13}(e)	2331	482	83	2311	357	2228	341	2176	2166	2165	2153	νSiH
ν_{14}(e)	2321	175	205	2304	110	2225	109	2167	2159	2163		νSiH
ν_4(a)	2311	4	60	2298	5	2217	1	2158	2153	2156		νSiH
ν_{15}(e)	2316	158	81	2299	188	2217	171	2163	2154	2155		νSiH
ν_{16}(e)	1160	160	5	1083	148	1077	95	1059	1049	1052	1024	δCH, $\nu_{as}CSi_3$
ν_5(a)	1081	48	3	1024	49	985	21	983	975	976	969	$\delta_s SiH_3$
ν_6(a)	1051	192	1	1007	143	969	123	956	959	960		$\delta_{as}'SiH_3$
ν_{17}(e)	1047	198	76	1002	91	963	37	952	954	954	939	$\delta_{as}'SiH_3$, $\delta_{as}''SiH_3$
ν_{18}(e)	1042	236	23	998	270	961	230	948	950	952		$\delta_{as}''SiH_3$, $\delta_{as}'SiH_3$
ν_7(a)	1033	0	8	988	1	953	1	939	940	943		$\delta_{as}''SiH_3$
ν_{19}(e)	1019	891	29	968	757	929	691	927	921	920	908	$\delta_s SiH_3$
ν_{20}(e)	891	294	15	860	258	833	239	842	840	833	826	$\nu_{as}CSi_3$, $\rho''SiH_3$
ν_8(a)	864	171	6	822	142	798	130	811	817	808	783	$\rho'SiH_3$
ν_{21}(e)	678	6	34	656	3	634	4	637	640	633		$\rho''SiH_3$
ν_9(a)	655	0	0	619	1	599	0	587	587	577		$\rho''SiH_3$, $\nu_{as}CSi_3$
ν_{22}(e)	627	1	11	592	2	578	0	585	584	581		$\rho'SiH_3$
ν_{10}(a)	487	2	22	488	2	465	2	472	477	472		$\nu_s CSi_3$
ν_{11}(a)	229	2	1	213	2	213	2	218	218	215		$\delta_s CSi_3$, $\rho'SiH_3$
ν_{23}(e)	177	1	0	163	1	168	1	168	165	170		$\delta_{as}CSi_3$
ν_{24}(e)	111	0	0	115	0	106	0	104	110	103		τSiH_3
ν_{12}(a)	109	0	0	130	0	76	0	113	178	74		τSiH_3

[a] QC frequency (cm^{-1}), unscaled or scaled. [b] QC infrared intensity (km mol^{-1}). [c] QC Raman scattering activity ($Å^4$ amu^{-1}). [d] Reference 3, "film". [e] Weak bands reported[3] at 2957, 2925, and 2855 cm^{-1} are likely to be combinations or overtones.

TABLE 7: Unscaled and Scaled Vibrational Data for TTMS

	HF/tz			MP2/tz		B3LYP/tz		HF/tz	MP2/tz	B3LYP/tz	obsd	
mode	ν_{unsc}[a]	A[b]	R[c]	ν_{unsc}[a]	A[b]	ν_{unsc}[a]	A[b]	ν_{sc}[a]	ν_{sc}[a]	ν_{sc}[a]	ν_{obsd}[d]	motion
ν_1(a)	2346	0	890	2309	0	2229	0	2191	2164	2167		νSiH
ν_9(t)	2330	1199	104	2307	1035	2228	318	2176	2162	2166		νSiH
ν_5(e)	2320	0	178	2297	0	2222	0	2171	2153	2160	2155s	νSiH
ν_{10}(t)	2325	302	221	2303	0	2218	0	2167	2158	2156		νSiH
ν_{11}(t)	2314	1	118	2295	138	2215	144	2161	2151	2153		νSiH
ν_2(a)	1097	0	1	1035	0	992	0	998	986	983		$\delta_s SiH_3$
ν_{12}(t)	1049	793	0	1001	274	964	391	954	953	955		$\delta_{as}SiH_3$
ν_6(e)	1049	0	81	1000	0	962	0	954	952	953		$\delta_{as}"SiH_3$
ν_{13}(t)	1034	25	20	986	4	950	6	941	939	941	916s	$\delta_{as}SiH_3$
ν_{14}(t)	1025	992	51	970	857	929	865	932	924	921	883m	$\delta_s SiH_3$
ν_{15}(t)	966	1061	0	933	1001	893	790	913	911	893	798vw	$\nu_{as}CSi_4$
ν_7(e)	758	0	39	720	0	694	0	702	702	690		ρSiH_3
ν_{16}(t)	663	5	1	629	5	604	6	614	614	601		ρSiH_3
ν_{17}(t)	632	5	35	612	0	584	3	586	597	581		ρSiH_3
ν_3(a)	416	0	18	412	0	395	0	403	403	400		$\nu_s CSi_4$
ν_{18}(t)	204	4	0	187	4	180	3	194	190	181		δCSi_4
ν_8(e)	156	0	1	145	0	139	0	148	147	141		δCSi_4
ν_4(a)	189	0	0	193	0	135	0	196	264	131		τSiH_3
ν_{19}(t)	150	1	1	153	0	120	1	140	146	117		τSiH_3

[a] QC frequency (cm^{-1}), unscaled or scaled. [b] QC infrared intensity (km mol^{-1}). [c] QC Raman scattering activity ($Å^4$ amu^{-1}). [d] Reference 2.

represents an in-phase rocking motion of the silyl groups, it has been taken to correspond with the A_2 motion in DSM. In fact, only one silyl rocking band has been observed, at 783 cm^{-1}, which must be due to ν_8(a). The best prediction for this band (808 cm^{-1}, B3LYP) is still 25 cm^{-1} too high.

A major difference in predicted values occurs for the A species silyl torsion mode ν_{12}. The distinction noted above between unscaled values from the HF, MP2, and B3LYP calculations is greatly exaggerated by the transfer of scale factors from DSM. The MP2/tz value rises from 115 to 178 cm^{-1}, while the corresponding HF and B3LYP values are hardly affected, at 113 and 74 cm^{-1}, respectively. Scale factor transfer for this mode therefore lacks plausibility. However, the E mode ν_{24} is very little affected by any transfer from DSM.

TTSM. The adjusted TTSM frequencies given in Table 7 were obtained by applying to the unscaled TTSM frequencies, also shown, the ratios of the scaled to unscaled frequency for similar modes in TSM. For the νSiH, δSiH_3, ρSiH_3, and δSiCSi modes, in each type of motion, the mean of the ratios found in TSM was applied. Error due to this approximation is most likely to occur in the prediction of the TTSM silyl rocking frequencies because the ratios of scaled to unscaled frequency for ν_8, ν_9, and ν_{21} in TSM differed significantly from each other. Similar differences would be expected in the ρSiH_3 modes of TTSM, but it was not clear which, if any, of the TTSM rocking modes corresponded with the three TSM motions. Only an average frequency ratio could therefore be applied.

Application of the TSM ratio for the torsional mode ν_{12}(a) (which embodies the DSM A_2 scale factor) to the unscaled value of ν_4(a) in TTSM gives from the MP2/tz result an adjusted value of 264 cm^{-1}, which seems far too high. This again suggests that the DSM torsional scale factors are not transferable.

TABLE 8: Comparison of QC Data for Isolated SiH Stretching Frequencies in TSM (C_3) and TTSM (T)

			sv			tz		
level	compound	terminal atom(s)[a]	ν, $\Delta\nu$[b]	A, ΔA[c]	R, ΔR[d]	ν, $\Delta\nu$[b]	A, ΔA[c]	R, ΔR[d]
HF	TSM	H^a	2370.6	165.9	86.5	2323.8	123.9	107.8
	TSM	H^b-H^a	2.1	32.6	36.4	4.2	26.6	42.9
	TSM	H^c-H^a	−4.0	32.7	31.3	−4.8	26.2	34.8
	TSM	average	2370.0	187.7	109.1	2323.6	141.6	136.2
	TTSM	H	2371.1	173.6	106.4	2324.3	129.1	127.5
MP2	TSM	H^a	2307.8	112.3	na	2306.0	92.9	na
	TSM	H^b-H^a	−0.4	34.2	na	5.1	na	na
	TSM	H^c-H^a	−7.8	32.5	na	−6.1	na	na
	TSM	average	2305.1	134.5	na	2305.7	na	na
	TTSM	H	2301.1	122.5	na	na	na	na
B3LYP	TSM	H^a	2248.7	111.4	na	2227.5	86.9	na
	TSM	H^b-H^a	−4.5	31.85	na	−1.5	26.7	na
	TSM	H^c-H^a	−9.8	30.96	na	−8.3	25.7	na
	TSM	average	2243.9	132.3	na	2224.2	104.4	na
	TTSM	H	2241.9	121.2	na	2221.3	94.1	na

[a] In Figure 1, H(6), H(9), and H(12) are H^a; H(7), H(10), and H(13) are H^b; while H(8), H(11), and H(14) are H^c. [b] Frequency or frequency shift (cm^{-1}). [c] Infrared intensity (km mol^{-1}); na = not available. [d] Raman scattering activity ($Å^4$ amu^{-1}).

TABLE 9: Comparison of Electrical Properties Associated with the Hydrogen Atom in the Si−H Bond in Some Silyl Compounds, from B3LYP/tz Calculations

compound/bond[a]	A_{obsd}[b]	A_{calcd}[c]	A_{obsd}/A_{calcd}	$\partial\mu/\partial r$[d]	θ[e]	$\bar{p}_\perp$[f]	$\bar{p}_A$[g]	χ[h]	q[i]
SiH_4[j]	70(1)	94.9	0.74	−0.287	0.0	−0.226	−0.246	0.248	−0.126
Si_2H_6[j]	72(4)	93.0	0.77	−0.293	9.1	−0.235	−0.253	0.262	−0.114
SiH_3CH_3[j]	102(5)	122.7	0.83	−0.329	4.8	−0.251	−0.277	0.280	−0.139
DSM/H^s[j]		136.9		−0.353	8.4	−0.254	−0.285	0.296	−0.133
DSM/H^a[j]		103.7		−0.300	0.4, 8.8	−0.248	−0.264	0.268	−0.132
DSM average[j]	90(3)	114.8	0.78						
TSM/H^a		86.9		−0.272	3.9, 9.1, 9.9	−0.240	−0.249	0.253	−0.122
TSM/H^b		113.6		−0.318	4.6, 10.1, 11.1	−0.244	−0.267	0.276	−0.123
TSM/H^c		112.6		−0.317	1.8, 10.4, 10.6	−0.246	−0.268	0.277	−0.128
TSM average	[81][k]	104.4	[0.78][k]						
TTSM	[73][k]	94.1	[0.78][k]	−0.210	13.5, 2.6, 13.7	−0.247	−0.251	0.259	−0.116

[a] This work, except where otherwise indicated. [b] Infrared intensity (km mol^{-1}) measured in the parent compound, divided by the number of SiH bonds. [c] Infrared intensity (km mol^{-1}) for the ν^{is}SiH band. This differs slightly from the calculated value in the parent molecule divided by the number of SiH bonds.[4] [d] Dipole derivative (e) with respect to SH bond stretching. [e] Angle (deg) between $\partial\mu/\partial r$ and the SiH bond. [f] Mean bending atomic charge (e), $= (p_{xx} + p_{yy})/2$, when the z axis lies along the Si−H bond.[16] [g] Mean atomic charge (e), $= (p_{xx} + p_{yy} + p_{zz})/3$. [h] King atomic charge (e). [i] Mulliken charge (e). [j] Reference 4. [k] Estimate.

Elsewhere, in addition to similar differences in prediction for silyl stretching and rocking modes to TSM, the three models disagree significantly on the positions of the $\delta_s SiH_3$ mode ν_2, the SiC stretching mode ν_{15}, and the skeletal mode ν_{18}.

The little information available on the observed spectrum (Table 7) shows a marked disagreement with the predicted frequencies in the 900 cm^{-1} region, which seems outside the likely range of gas−liquid frequency shifts. Vapor phase spectra will be needed to clarify the situation. From the considerations below, the overall observed infrared intensity of the νSiH bands should be about 880 km mol^{-1}.

Isolated SiH Stretching Bands and Electrical Properties of the H(Si) Atoms. Data relating to the frequencies and intensities associated with the SiH stretching modes of the species $(SiHD_2)(SiD_3)_2CH$ and $(SiHD_2)(SiD_3)_3C$ are displayed in Table 8. For TSM, it is useful to quote for the $Si-H^b$ and $Si-H^c$ bonds the differences they exhibit from the $Si-H^a$ bond. This highlights the comparatively small changes in frequency but quite large changes in both infrared intensity and Raman scattering activity, which are predicted uniformly by all levels of theory for the different types of Si−H bond present. Markedly reduced intensities are associated with the $Si-H^a$ bonds, which are those most nearly antiperiplanar to the C−H bond (dihedral angle ~160°).

The average TSM frequency is very close to the TTSM value. However, there is a modest fall in both infrared and Raman intensity from TSM to TTSM.

It is instructive to compare electrical properties of the H(Si) atoms across a range of SiH-containing compounds, computed at the same level of theory, as in Table 9. Experimental measurements of infrared intensity in the SiH stretching regions of silane,[12] disilane,[13] methylsilane,[13] and disilylmethane[13] are available, which permit a comparison of the observed (average) intensity per Si−H bond with that from a B3LYP/tz calculation. The ratio of experimental to theoretical value lies in the range 0.74 to 0.83. From this one can estimate the experimental intensities for TSM (average) and TTSM, which after multiplication by the number of Si−H bonds yields the estimates quoted above for the SiH stretching regions of the two molecules. The chemical trend is for an increase in νSiH intensity with methyl substitution, as in MS. The normal inductive effect of methyl will be to increase the negative charge on the H(Si) atoms, as shown by the Mulliken charges. That this effect is due primarily to the methyl C−H bonds is suggested by the progressive diminution of the intensity increase in DSM and TSM until in TTSM the value is essentially back to that found in silane or disilane. This intensity sequence is of course mirrored by the values of $\partial\mu/\partial r$ for the Si−H bond; however, the direction θ of $\partial\mu/\partial r$ is variable and tends to increase slightly with the number of silyl groups.

Isolated CH Stretching Bands and Electrical Properties of the H(C) Atoms. These are compared for the C−H bonds in methane (M), MS, DSM, and TMS in Table 10. A fall in infrared intensity per C−H bond with increasing silyl substitu-

TABLE 10: CH Stretching Intensities A and Electrical Properties Associated with the Hydrogen Atom in C−H Bonds in Methane (M), Methylsilane (MS), DSM, and TSM from B3LYP/tz Calculations

property	M	MS	DSM[a]	TSM[a]
$A(\nu\mathrm{CH})_{\mathrm{av.expt}}$[b]	16.4(1)[c]	7.5(2)[d]	2.7(2)[d]	[0.5][e]
$A(\nu\mathrm{CH})_{\mathrm{av.calcd}}$[b]	21.0[f]	9.2[f]	3.3[g]	0.6
$A(\nu^{\mathrm{is}}\mathrm{CH})_{\mathrm{calcd}}$[h]	21.5[a]	9.0[a]	3.2	0.6
$A_{\mathrm{av.expt}}/A_{\mathrm{av\cdot calcd}}$	0.78	0.82	0.82	[0.82][e]
$\partial\mu/\partial\mathrm{r}^i$	−0.151[f]	−0.118[f]	−0.089	−0.064
θ^j	0.0	9.6[f]	8.7	0.0
$\bar{p}_\perp{}^k$	0.077[f]	0.071[f]	0.063	0.049
$\bar{p}_\mathrm{A}{}^l$	0.001[a]	0.009[f]	0.013	0.011
χ^m	0.108[f]	0.095[f]	0.079	0.054
q^n	0.109[f]	0.135[f]	0.162	0.198

[a] This work except where otherwise indicated. [b] Average infrared intensity (km mol^{-1}) observed (obsd) or calculated (calcd) in the νCH region of the parent molecule, divided by the number of CH bonds. [c] References 14 and 15. [d] Reference 13. [e] Estimate. [f] Reference 5. [g] Reference 4. [h] Infrared intensity (km mol^{-1}) for the ν^{is}CH band. [i] Dipole derivative with respect to stretching of the CH bond (e). [j] Angle (deg) between $\partial\mu/\partial r$ and the C−H bond. [k] Mean bending atomic charge (e), $= (p_{xx} + p_{yy})/2$, when the z axis lies along the C−H bond.[16] [l] Mean atomic charge (e), $= (p_{xx} + p_{yy} + p_{zz})/3$. [m] King atomic charge (e). [n] Mulliken charge (e).

tion is found both experimentally and theoretically, the ratio of the two quantities being similar to that found for SiH stretching. An estimate of 0.82 for this ratio in TSM leads to the prediction above of an observed intensity for CH stretching of 0.5 km mol^{-1}.

As is usual for C−H bonds, $\partial\mu/\partial r$ is negative, attributed to a dominating charge flux term.[16] The fall in this negative value in the sequence M-MS-DSM-TSM follows nicely the increase in the static positive charge on the H atom, as given by the Mulliken charge, and is attributable to the electron-withdrawing effect of a silyl group. However, it might have been expected that the mean bending moment $\bar{p}_\perp$,[17] which, as usual, is positive, would increase as the Mulliken charge increased. Instead, $\bar{p}_\perp$ diminishes. CH bending in these molecules is therefore likely to involve movement of charge elsewhere in the molecule.

Conclusions

QC calculations confirm that the silyl groups in the equilibrium forms of TSM and TTSM are twisted by up to 20° from the corresponding fully staggered configurations. The barrier between equilibrium and staggered forms, together with the associated torsional frequency, is significantly greater from MP2 or HF calculations than from B3LYP ones. Likely sources of these differences are the longer bond lengths and nonbonded H···H distances yielded by the DFT method.

Vibration frequencies of TSM are predicted by transferring scale factors from DSM and compared with scanty experimental data. The transfer procedure is considered to be dubious in the case of δCH and silyl rocking modes and unacceptable for torsional frequencies. A simpler scaling procedure used in TTSM encounters the same difficulties. IR intensities of νCH and νSiH bands in TSM and TTSM are estimated to be 0.5, 730, and 880 km mol^{-1}, respectively. The predicted position (2895 cm^{-1}) and IR intensity of the νCH band in TSM both suggest that this band has not yet been observed. Further experimental work on the vibrational spectra of TSM and TTSM is urgently needed.

Calculated changes in the electrical properties of the CH and SiH bonds across a series of silyl-containing compounds are explained in terms of conventional inductive effects.

Acknowledgment. Professor D. W. H. Rankin and Dr. S. L. Hinchley are warmly thanked for making available the Edinburgh ab initio facility for running the Gaussian 98 program. The U.K. Computational Chemistry Facility, administered by the Department of Chemistry, King's College London, Strand, London WC2R 2LS, is thanked for computing time on Columbus.

Supporting Information Available: Symmetry coordinates for DSM (Table 1S), fully staggered structures calculated for TSM (C_{3v}) (Table 2S) and TTSM (T_d) (Table 3S), and staggered and eclipsed structures calculated for methylsilane (Table 4S). This material is available free of charge via the Internet at http://pubs.acs.org.

References and Notes

(1) Schmidbaur, H.; Zech, J.; Rankin, D. W. H.; Robertson, H. E. *Chem. Ber*. **1991**, *124*, 1953.
(2) Hager, R.; Steigelmann, O.; Möller, G.; Schmidbaur, H.; Robertson, H. E.; Rankin, D. W. H. *Angew. Chem., Int. Ed. Engl.* **1990**, *29*, 201.
(3) Hager, R.; Steigelmann, O.; Müller, G.; Schmidbaur, H. *Chem. Ber*. **1989**, *122*, 2115.
(4) McKean, D. C. *J. Phys. Chem*. *A* **2003**, *107*, 6538.
(5) Mathews, S.; Duncan, J. L.; McKean, D. C.; Smart, B. A. *J. Mol. Struct*. **1997**, *413*−*414*, 553.
(6) Frisch, M. J.; Trucks, G. W.; Schlegel, H. B.; Scuseria, G. E.; Robb, M. A.; Cheeseman, J. R.; Zakrzewski, V. G.; Montgomery, J. A., Jr.; Stratmann, R. E.; Burant, J. C.; Dapprich, S.; Millam, J. M.; Daniels, A. D.; Kudin, K. N.; Strain, M. C.; Farkas, O.; Tomasi, J.; Barone, V.; Cossi, M.; Cammi, R.; Mennucci, B.; Pomelli, C.; Adamo, C.; Clifford, S.; Ochterski, J.; Petersson, G. A.; Ayala, P. Y.; Cui, Q.; Morokuma, K.; Malick, D. K.; Rabuck, A. D.; Raghavachari, K.; Foresman, J. B.; Cioslowski, J.; Ortiz, J. V.; Stefanov, B. B.; Liu, G.; Liashenko, A.; Piskorz, P.; Komaromi, I.; Gomperts, R.; Martin, R. L.; Fox, D. J.; Keith, T.; Al-Laham, M. A.; Peng, C. Y.; Nanayakkara, A.; Gonzalez, C.; Challacombe, M.; Gill, P. M. W.; Johnson, B. G.; Chen, W.; Wong, M. W.; Andres, J. L.; Head-Gordon, M.; Replogle, E. S.; Pople, J. A. *Gaussian 98*, revision A.7; Gaussian, Inc.: Pittsburgh, PA, 1998.
(7) Hedberg, L.; Mills, I. M. *J. Mol. Spectrosc*. **2000**, *203*, 82.
(8) Cyvin, S. J.; Mooney, R. W.; Brunvoll, J.; Kristiansen, L. A. *Acta Chem. Scand*. **1965**, *19*, 1031.
(9) McKean, D, C.; Torto, I. *Spectrochim. Acta* **2001**, *57A*, 1725.
(10) Schleyer, P. v. R.; Kaupp, M.; Hampel, F.; Bremer, M.; Mislow, K. *J. Am. Chem. Soc*. **1992**, *114*, 6791.
(11) Mastryukov, V. S.; Boggs, J. E.; Samdal, S. *J. Mol. Struct*. **1993**, *283*, 199.
(12) Coats, A. M.; McKean, D. C.; Steele, D. *J. Mol. Struct*. **1994**, *320*, 269.
(13) McKean, D. C.; Coats, A. M. *Spectrochim. Acta A*, to be published.
(14) Newton, J. H.; Person, W. B. *J. Phys. Chem*. **1978**, *82*, 226.
(15) Bode, J. H. G.; Smit, W. M. A. *J. Phys. Chem*. **1980**, *84*, 198.
(16) cf. Gussoni, M.; Jona, P.; Zerbi, G. *J. Chem. Phys*. **1983**, *78*, 6802.
(17) McKean, D. C.; Torto, I. *J. Mol. Spectrosc*. **2002**, *216*, 363.